

An Automated Quantitative Analysis of Ventilation-Perfusion Lung Scintigrams

Graham H. Burton, Phillip Vernon, and W. Anthony Seed

Charing Cross Hospital, London

We have devised an automated computer analysis of ventilation (Kr-81m) and perfusion (Tc-99m) lung images that produces a graphical image of the distribution of ventilation and perfusion, and of ventilation-perfusion ratios. The analysis has overcome the following problems: the identification of the midline between two lungs and the lung boundaries, the exclusion of extrapulmonary radioactivity, the superimposition of lung images of different sizes, and the format for presentation of the data. Therefore, lung images of different sizes and shapes may be compared with each other. The analysis has been used to develop normal ranges from 55 volunteers. Comparison of younger and older age groups of men and women show small but significant differences in the distribution of ventilation and perfusion, but no differences in ventilation-perfusion ratios. Examples are presented to demonstrate that the technique can discriminate between normal and abnormal scintigrams. The analysis of serial images from one individual shows high reproducibility.

J Nucl Med 25: 564-570, 1984

Diagnostic analysis of ventilation and perfusion lung images is commonly based on the visual interpretation of the scintigrams. Although observer interpretation has been aided by the development of functional images (1) and images highlighting areas of abnormal ventilation-perfusion ratios (2), these techniques have several disadvantages. First, the images have not been assessed by reference to normal ranges; second, the images still require visual interpretation subject to inter- and intraobserver bias (3) and third, they are not amenable to comparison with physiological indices of ventilation-perfusion matching because they are not quantitative.

We have therefore devised an automated computerized analysis of ventilation-perfusion lung images that provides quantitative information, permits comparison of images between subjects, and allows the establishment of normal ranges. The analysis presents data on ventilation, perfusion, and their relationship in a graphical

form, and calculates numerical indices of abnormality when any of these parameters falls outside normal limits.

METHOD

The ventilation-perfusion lung scintigram. An intravenous injection of 2 mCi of Tc-99m-labeled macroaggregated albumin was given with the subject supine and breathing deeply. The subject was then seated in front of a wide-field-of-view gamma camera and asked to breathe room air normally through a disposable face mask. Pictures of the technetium distribution were then made by accumulating 300,000 counts with the window of the camera set for the 140-keV gamma peak. A constant supply of krypton-81m was then added to the subject's inspired air by passing air at a flow rate of 6 l/min through a rubidium generator (4,5). Three hundred thousand counts were then collected with the camera window set for the 190-keV gamma energy of Kr-81m.

Perfusion and ventilation images were recorded in the

Received Aug. 17, 1983; revision accepted Dec. 29, 1983.

For reprints contact: G. Burton, BSc MRCP, Dept. Medicine, Charing Cross Hospital, Fulham Palace Rd., London W6 8RF.

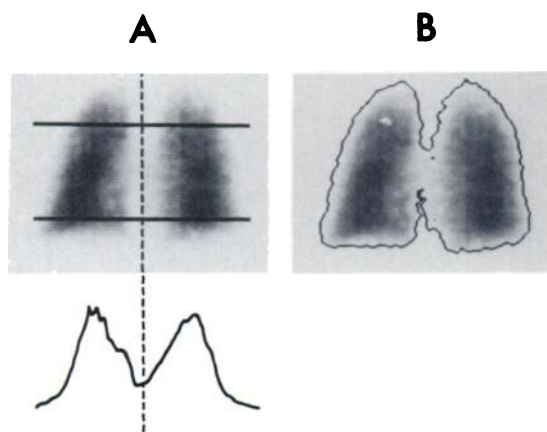


FIG. 1. Analysis of normal ventilation-perfusion lung study. A: Posterior perfusion image. Summed counts between two horizontal lines are plotted below scintigram. Computer identifies midline in position of dotted line. B: Same scintigram showing 18% contour line to define lung boundaries.

anterior, posterior, right and left lateral (or right and left posterior oblique) positions, and the counts for each view were stored in a computer in a 64×64 matrix. The matrix is a table in which each entry is the number of gamma rays detected in a 6- by 6-mm area of the gamma camera. The area covered by the matrix is larger than that of the lungs.

The computer analysis. The program was confined to the analysis of data stored from the posterior ventilation and perfusion images. Statistical fluctuations in the counts recorded in each cell were first reduced by a nine-point smoothing process (6). Thereafter, the program was concerned with the definition of the boundaries of the lungs, scaling of the lung images to a standard size, graphical representation of these lung images, and comparison between ventilation and perfusion. The procedure was entirely automatic and involved no operator intervention.

The midline between right and left lungs was first defined by summing vertically the counts in the array of 64×64 cells and identifying the minimum point between two maxima (Fig. 1A). The column of cells with minimum counts was then set to zero and taken as the midline.

The edges of the lungs, one on either side of the midline, were next defined. It was established that a contour drawn at 18% of the maximum counts per cell (Fig. 1B) produced a reliable boundary (see Discussion). All counts outside these boundaries on either side of the midline were therefore excluded. This procedure did not always establish a single continuous area representing the lung on either side of the midline; separate areas of high counts attributable to face mask, trachea, liver, or spleen were sometimes present. In such cases the largest area on either side of the midline was designated as the lung, and unconnected regions of high counts were set to zero.

The length of each lung from top to bottom was then defined by the number of cells on the vertical axis still containing counts. The lengths of the ventilation and perfusion images of one lung were compared, and if they differed, it was assumed that the longer represented the true lung size. The other lung was treated in the same way, and finally the left and right lungs were compared and the longer lung assumed to represent the true lung size. This procedure was chosen, after examination of a number of alternatives, as the most satisfactory in the analysis of images from patients with gross disease (see Discussion).

The program then normalized the vertical axis of each lung to a common length of 50 arbitrary units, and derived numbers at each of the 50 points by linear interpolation. The horizontally summed counts in each row were then plotted (as fractions of the total of left and right lung counts) on the horizontal axis of a graph, with lung length as the vertical axis (Figs. 2A & B).

Both perfusion and ventilation images were processed in this manner. The ventilation and perfusion activities at each of the 50 points down each lung were then compared in two ways. First, a ventilation-perfusion difference ($V-Q$) was calculated by direct subtraction at each vertical point in each lung, then plotted with lung length as ordinate and count difference as abscissa (Fig. 2C). Second, a direct ratio (V/Q) was calculated and plotted (Fig. 2D).

Normal subjects. Fifty-five life-long nonsmokers, drawn from hospital staff, students, and preoperative surgical patients, were selected as normal subjects. Other

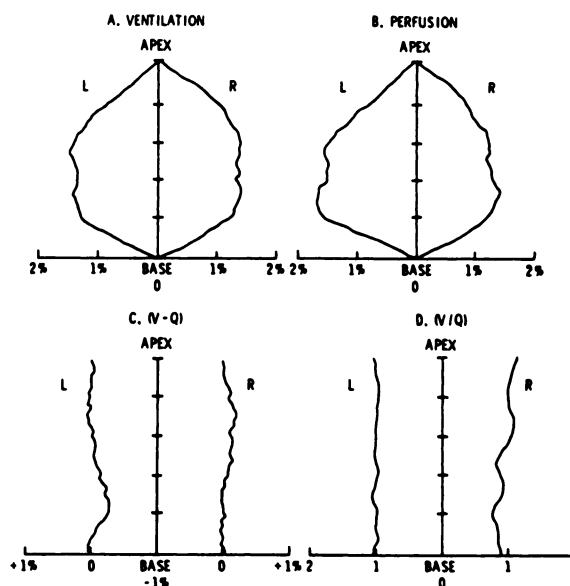


FIG. 2. Computer analysis of (A) ventilation and (B) perfusion images from individual, plotting percentage of total counts from both lungs against normalized lung length. C: Ventilation minus perfusion ($V-Q$) plotted as differences between A and B against normalized lung length. D: Ventilation-perfusion ratio (V/Q), derived from A and B, plotted against normalized lung length.

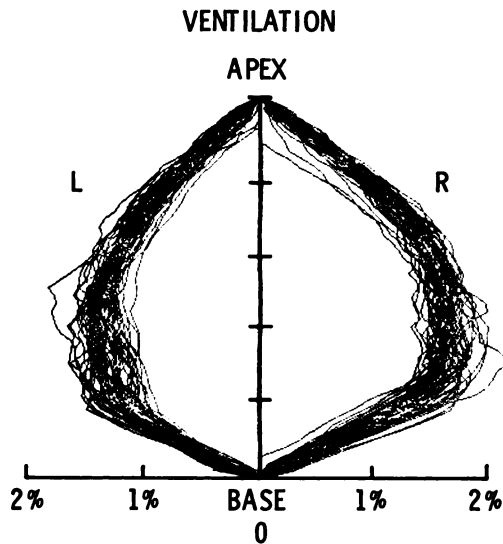


FIG. 3. Superimposed ventilation analyses from 55 normal subjects, plotted as Fig. 2A.

criteria included a negative history for respiratory disease, normal airways function (forced expiratory volume in 1 sec and forced vital capacity), and a normal chest radiograph, taken within 3 mo of the study. All had a ventilation-perfusion lung study performed in the way described.

From these images, normal ranges for the distribution of ventilation and perfusion were constructed by deriving the mean and standard deviation for each of the fifty points down the lung. This process was repeated for the (V-Q) and (V/Q) points and the values of mean and mean ± 2 s.d. for the ventilation, perfusion, (V-Q) and (V/Q) ratio were stored in the computer.

In addition, scintigrams processed in the same way for subgroups based on age and sex were examined. The subjects were divided into four groups: men under 30 yr of age (N = 17, mean age 24.2, range 19.1 to 28.6); women under 30 yr of age (N = 16, mean age 23.8, range 19.8 to 29.6); men over 30 yr of age (N = 9, mean age 50.0, range 31.5 to 71.5); and women over 30 yr of age (N = 13, mean age 45.4, range 31.8 to 59.8). The mean values for each of the points down the lung for these four subgroups were compared using an unpaired t-test. A difference was considered significant if the p value obtained was less than 5% ($p < 0.05$).

The method of analysis has also been applied to a study of patients with a variety of lung diseases. Here, in addition to provision of graphical data, the computer produces numerical values for the extent of any abnormality of V, Q, or the derived indices. These values are calculated as the area bounded by the abnormal graph and the limit of the normal range (defined as 2 s.d. from the mean for the age- and sex-matched group of normal subjects). In Fig. 7, for example, the abnormal areas are those contained between the patient's graph and the limit of the (stippled) normal range.

Copies of the computer program, written in FORTRAN, and the data on normal ranges are available from the authors.

RESULTS

Normal subjects. The individual analyses of the ventilation images from the 55 normal subjects are shown superimposed in Fig. 3. The coefficients of variation of the values obtained at each point down the lungs range between 7% and 14% except for the two apical and two basal points, where the CV reaches values between 20% and 40%. Analysis of the perfusion images gives similar coefficients of variation. The values calculated at each of the fifty points down the left and right lungs were normally distributed for the ventilation and perfusion images. Figures 4A and 4B show the ventilation and perfusion scintigrams as the mean ± 2 s.d. at each point for the 55 normal subjects. The calculations of ventilation minus perfusion (V-Q) and ventilation-perfusion ratio (V/Q) are similarly plotted in Figs. 4C and 4D.

Within the normal population, differences were found between subgroups on the basis of both age and sex. In some cases the differences concerned ventilation only, in others ventilation and perfusion. Details are given in Table 1 and summarized below in terms of percentage differences for the zone of the lung involved. Illustrative examples are shown in Fig. 5. In no case were there significant differences in ventilation-perfusion relationships.

Differences between sexes. The group of younger men had 11% less ventilation in the upper zone of the right lung than the group of younger women (Fig. 5A). A 9%

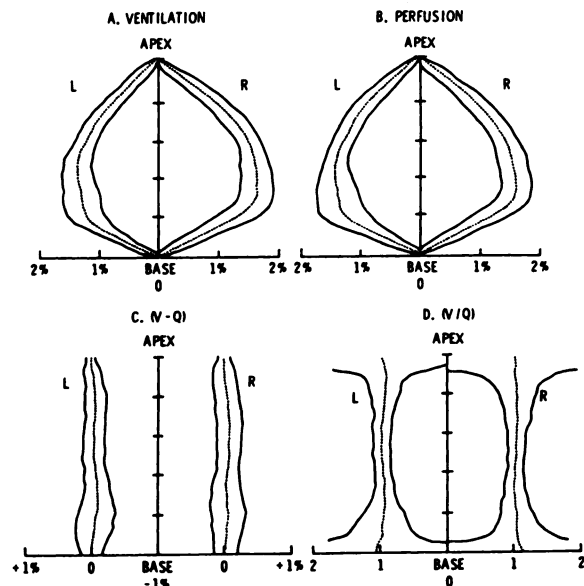


FIG. 4. Mean values (dotted lines) ± 2 s.d. (solid lines) from 55 normal subjects for (A) ventilation and (B) perfusion images, with (C) ventilation minus perfusion (V-Q) and (D) ventilation-perfusion ratios (V/Q).

TABLE 1. DISTRIBUTION OF ACTIVITY IN THE LUNGS OF THE FOUR GROUPS OF NORMAL SUBJECTS

		Men <30 yr	Women <30 yr	Men >30 yr	Women >30 yr
Ventilation					
Left	U*	12.1	12.6	11.0	11.7
	M	21.7	21.3	20.8	19.7
	L	13.8	13.0	13.5	11.7
Right	U	13.6	15.3	14.2	15.7
	M	24.7	24.9	26.1	26.5
	L	14.1	12.9	14.4	14.7
Perfusion					
Left	U	12.9	13.5	12.1	12.9
	M	22.4	22.7	22.1	20.8
	L	14.2	13.7	13.9	12.3
Right	U	13.2	13.4	14.0	14.6
	M	23.8	24.0	24.8	25.2
	L	13.5	12.7	13.1	14.2

* U = upper, M = middle, L = lower zones of the lung.
Values represent percentages of total activity of both lungs.

difference was found between the groups of older men and women in the same area. In addition, the group of older men had 13% more ventilation and 12% more perfusion in the lower zone of the left lung than did the older women.

Differences between age groups. Older women had 12% more ventilation and 11% more perfusion than younger women in the lower zone of the right lung. Older women also had 10% less ventilation and 10% less perfusion than younger women in the lower zone of the left lung. The ventilation differences are illustrated in Fig. 5B.

Older men had 9% less ventilation in the upper zone of the left lung than did younger men.

Differences within a subject. Figure 6 shows the reproducibility of the method in one normal subject by

superimposing five lung images done over an 18-mo period.

Abnormal subjects. The technique is currently being applied in the study of a range of lung diseases, with the intention of testing its discriminant ability. Examples from patients with chronic obstructive airways disease (COAD) and pulmonary embolism are shown in Fig. 7.

In COAD (Fig. 7A) the analysis detects abnormal areas of both ventilation and perfusion in both lungs. Although the abnormalities in such images often appear on simple inspection to be matched, the analysis of (V-Q) in a large series of such cases has demonstrated widespread mismatching (Fig. 8).

In pulmonary embolism (Fig. 7B), ventilation lies within the normal range, but the analysis of perfusion detects two areas of underperfusion, misses a third small area at the left apex, and shows the relative overperfusion of the unaffected areas of both lungs. When matching

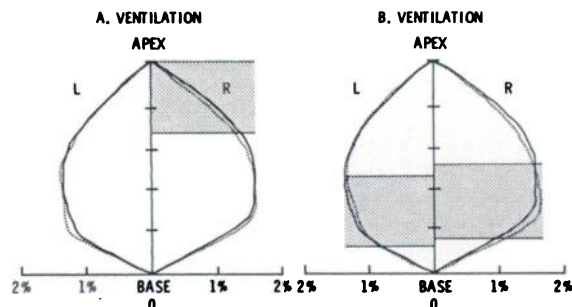


FIG. 5. Differences between normal subgroups, with stippling to show areas where differences between two groups reached significance. A: Mean data for ventilation images of group of younger women (solid line) and of younger men (dotted line). B: Mean data for ventilation images of group of younger women (solid line) and of older women (dotted line).

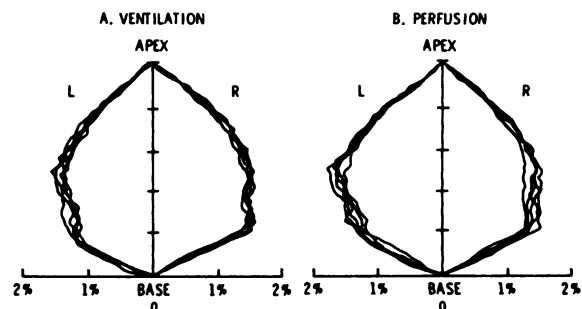


FIG. 6. Intrasubject variation. Five separate ventilation-perfusion lung studies in one subject, plotted as Fig. 2.

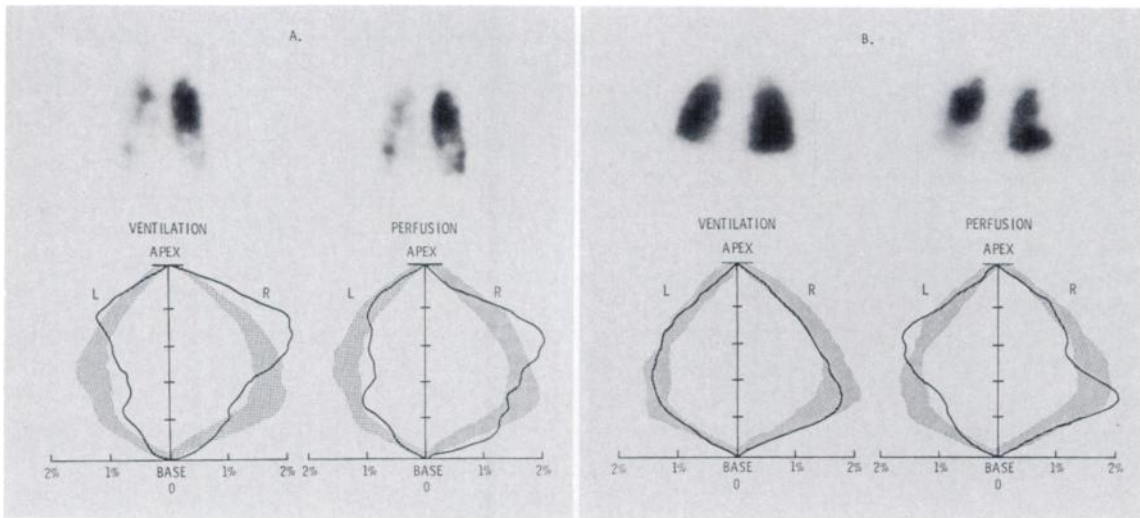


FIG. 7. Posterior ventilation and perfusion lung images (upper) and their computer analyses (lower, with age- and sex-matched normal ranges represented by stippling) in lung disease. A: In stable chronic obstructive airways disease (FEV_1/FVC ratio = 54%). B: In acute pulmonary embolism.

of ventilation and perfusion is examined, the technique appears to be sensitive in detecting underperfusion caused by the emboli (Fig. 9). Furthermore, the underperfusion score appears to correlate well with the severity of the embolism. Figure 10 presents data from a smaller group of patients who had arterial blood gases analyzed during the acute event. The partial pressure of oxygen

in arterial blood (pO_2), which has been shown to correlate closely with the severity of angiographic obstruction in acute pulmonary embolism (7), is plotted against the relative underperfusion score—i.e., the summed values of $(V-Q)$ falling above the upper limit of normal. Linear regression analysis reveals a highly significant inverse correlation ($r = -0.59, p < 0.01$).

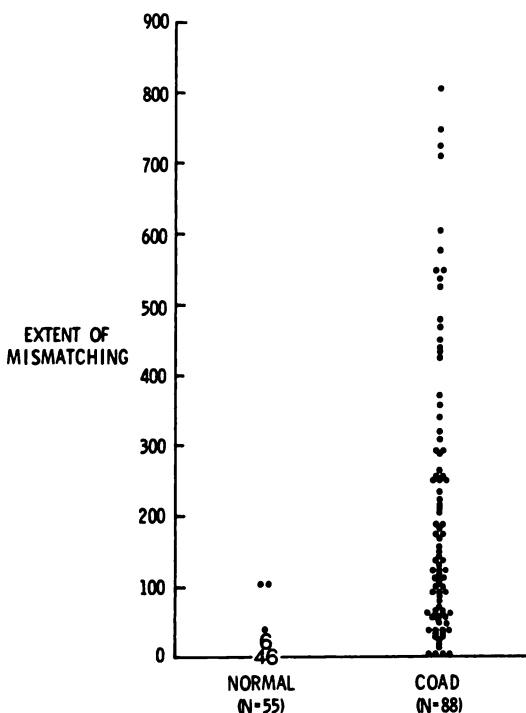


FIG. 8. Ability of method to detect mismatching between ventilation and perfusion. Ordinate shows summed computer-analysis score for high and low $(\dot{V} - \dot{Q})$ values in 55 normal subjects and in 88 patients with COAD of varying severity (FEV_1/FVC ratios from 25 to 80%).

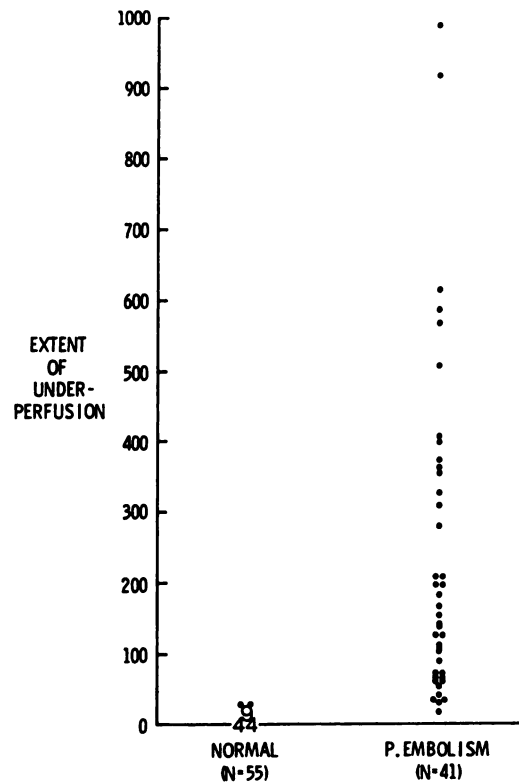


FIG. 9. Extent of underperfusion detected by computer analysis in 55 normal subjects and 41 cases of acute pulmonary embolism of varying severity.

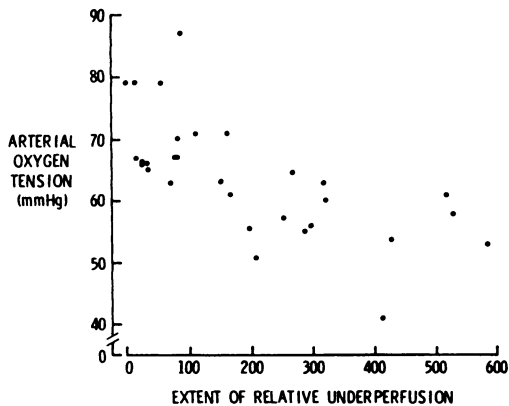


FIG. 10. Acute pulmonary embolism: arterial pO_2 (ordinate) against computed score for extent of relative underperfusion (abscissa). See text.

DISCUSSION

It has proved possible to automate the analysis of lung scintigrams. The technique, applied to 55 normal subjects, produces mean data with coefficients of variation of 7% to 14%, comparable to those for many respiratory function variables. Within a healthy individual (Fig. 6) the method is highly reproducible.

An obvious test of the method is to apply it to images from patients with lung disease. The precision and clinical usefulness of the method is the subject of a further study, but limited examples are presented here (Figs. 7-10). These are intended to illustrate that the technique can detect disturbances of ventilation and perfusion and quantify them. The ability of the technique to detect mismatching in COAD (Fig. 8) is reassuring, since independent physiological tests (blood-gas analysis and dead-space measurement) have established it as a feature of the disease. Similarly, the technique appears to have promise in quantification of pulmonary embolism (Fig. 10).

The principal purpose of the present study, however, is to evaluate the method of analysis, and in this context two points concerning the definition of the lung boundaries require comment. First, the position of the patient within the field of view of the gamma camera is not critical because both the midline and the lung boundaries are identified for each image. This removes the need for accurate repositioning if the images are repeated. Second, it is possible to compare lungs of different sizes and shapes because of the techniques used to identify lung boundaries and scale lung length.

The identification of the lung boundary involves an arbitrary choice of activity level. When the lung image is examined in a direction normal to its edge, the greatest rate of change of counts per pixel occurs where counts lie between 12% and 25% of the maximum. However, the greatest rate of change is not itself a convenient parameter because its definition requires considerable

smoothing and calculation. Instead, therefore, a single level of activity has been used. In normal subjects the contour lines are very close together, between 12% and 25%, and the midpoint (18%) has been arbitrarily chosen. The merits of the technique are: first, that all areas within the 18% contour are considered part of the lung, so an area of low count rate lying within the 18% contour will not be excluded; and second, that areas of high count rate not contiguous with the lung are excluded. The drawback is that ventilation or perfusion defects reaching out to the lung boundary will be excluded. For example, a peripheral pulmonary embolus reducing activity near the lung edge to 10% will be excluded from analysis, and this will have the effect of exaggerating the defect, in this case by 8%. In the worst case the severity of the defect, but not its extent, would be overestimated by 18%.

In normal subjects the four lung images show only small variations in length. This will not be true for abnormal images however, and if one lung image is shorter than the other due to disease, a procedure is needed to avoid masking the abnormality by scaling up the shorter lung. If the ventilation and perfusion images of a lung differ in size, the longer image is assumed to represent the real length. Similarly, if left and right lung images differ, it is assumed that the shorter lung is abnormal. The program compares the lengths of the four images and scales the longest to the standard length of 50 units. Each of the shorter images is then scaled proportionately. If differences in lung length are found, the final problem is in determining whether the length defect lies at the top or the bottom, or both, of the shorter lung. The program compares the apex and base positions on the matrix for the right and left lungs. If the bases have similar values and the apices differ, then the shorter lung has an apical defect. If the apices have similar values and the bases differ, the shorter lung has a basal defect. If both apices and bases differ, it is assumed that the shorter lung has two defects. Limits are set on this process so that minor (less than 10%) differences in lung lengths are not corrected.

The results from the analysis of 55 normal subjects demonstrate that the procedure has effectively minimized intersubject variations in size, shape, and position. However, the calculated (V/Q) ratios (Fig. 4D) show a wide range at the top and bottom of both lungs, because in these areas there are few counts and hence the error is large. Subtraction does not emphasize these errors, and therefore the (V-Q) analysis has a smaller scatter at the top and bottom (Fig. 4C).

Small but statistically significant differences in scintigrams have been found between the normal subgroups based on age and sex. Since these differences apply to both ventilation and perfusion images (i.e. there are no differences in (V/Q) ratios), they are probably due to differences in chest shape or, when they affect the left lung, heart size. These differences should be seen in the

context of the normal range for all 55 subjects; in no case did the results from a subgroup fall outside this normal range.

The lung-image analysis does not present conventional physiological data about ventilation-perfusion ratios. The method was devised to analyze lung images taken for diagnostic purposes with the perfusion image reflecting the distribution of blood in the supine lung and the ventilation image the distribution of ventilation in the erect lung. The majority of physiological studies present ventilation-perfusion relationships for the lung in a single posture and, moreover, ventilation and perfusion may be calibrated in absolute terms, expressed per unit of lung volume. Thus, it is difficult to compare our results precisely with data in the physiological literature, though it is predictable that with this imaging technique (which eliminates the perfusion gradient present in the upright lung) close correspondence between ventilation and perfusion can be expected.

It is possible, however, to use physiological principles to test the sensitivity of the method to disturbances of normal ventilation-perfusion relationships. The latter are common to a wide range of lung disease and produce arterial hypoxemia, which can be quantified by arterial blood-gas analysis. Such a study is currently in progress, as is the clinical evaluation of the usefulness of the

method in diagnostic nuclear medicine.

ACKNOWLEDGMENT

Dr. G. Burton was in receipt of a Charing Cross Hospital Trustees Clinical Research Fellowship during part of this work.

REFERENCES

1. ALPERT NM, MCKUSICK KA, CORREIA JA, et al: Initial assessment of a simple functional image of ventilation. *J Nucl Med* 17:88-92, 1976
2. ARNOLD JE, WILSON BC: Computer processing of perfusion, ventilation, and V/Q images to highlight pulmonary embolism. *Eur J Nucl Med* 6:309-315, 1981
3. HOEY JR, FARRER PA, ROSENTHALL LJ, et al: Interobserver and intraobserver variability in lung scan reading in suspected pulmonary embolism. *Clin Nucl Med* 11:508-513, 1980
4. JONES T, CLARK JC, HUGHES JM, et al: ^{81m}Kr generator and its uses in cardiopulmonary studies with the scintillation camera. *J Nucl Med* 11:118-124, 1970
5. FAZIO F, JONES T: Assessment of regional ventilation by continuous inhalation of radioactive krypton-81m. *Br Med J* 3:673-676, 1975
6. VERNON P, GLASS HI: Processing gamma-camera data obtained from an off-line system. In *Dynamic Studies with Radioisotopes in Medicine*. Vienna, IAEA, 1971, pp 133-143
7. MCINTYRE KM, SASAHARA AA: The hemodynamic response to pulmonary embolism in patients without prior cardiopulmonary disease. *Am J Cardiol* 28:288-294, 1971